Hindawi
International Journal of Geophysics
Volume 2019, Article ID 5057832, 13 pages
https://doi.org/10.1155/2019/5057832

Research Article

Contaminant Delineation of a Landfill Site Using Electrical Resistivity and Induced Polarization Methods in Alice, Eastern Cape, South Africa

S. Mepaiyeda ,[1] K. Madi,[2] O. Gwavava,[1] C. Baiyegunhi,[3] and L. Sigabi[1]

[1]*Department of Geology, University of Fort Hare, Private Bag X1314, Alice 5700, South Africa*
[2]*School of Biology and Environmental Sciences, University of Mpumalanga, Private Bag X11283, Mbombela, 1200, Mpumalanga, South Africa*
[3]*Department of Geology and Mining, University of Limpopo, Private Bag X1106, Sovenga 0727, South Africa*

Correspondence should be addressed to S. Mepaiyeda; 201714260@ufh.ac.za

Received 5 March 2019; Revised 5 June 2019; Accepted 21 August 2019; Published 22 December 2019

Academic Editor: Pantelis Soupios

A combination of electrical resistivity and induced polarization methods were applied to a solid waste landfill in Alice, Eastern Cape, South Africa to delineate the lithologic layers and locate possible leachate plumes. Resistivity and IP data were collected along six profiles; VES on two and the dipole-dipole configuration was used in the rest four. The result shows a 4-layered earth system with a shallow depth to the top of the bedrock (<10 m). Contaminants ranging from unsaturated waste with high ion content to dense aqueous phase liquid contaminants, characterized by low resistivity (34–80 Ohm-m) and low chargeability values (0.05–5.75 ms). The contamination was interpreted based on resistivity/IP anomalies considering the background geology. The shallow bedrock indicated a low risk to groundwater contamination because of its competent nature from its geology, and characteristic high resistivity values (≥1000 Ohm-m). However, the steep nature of the landfill terrain due to its location at the foot of a vertical slope favours the rapid migration of the contaminants into the immediate vicinity of the landfill. The construction of containment structures such as waste cells will help in enhancing effective waste management practices in the landfill.

1. Introduction

Landfills are common feature of the environment, especially in urban and highly populated cities where they have become a predominant means of waste disposal. In developing economies, unregulated landfills are commonly located adjacent to large cities, releasing leachate which contains contaminants, thereby polluting underlying aquifers [1]. Municipal solid waste landfills/dumpsites have been identified as a major environmental problem when located in proximity to inhabited areas [2]. Most times, landfills were initially sited far from developed areas. Increasing population and urbanization have led to the use of land in the vicinity of landfills either as public or residential. This expose human and animals to environmental hazards such as percolation of polluted leachate into the shallow aquifers that serves as a major source of water supply in developing countries such as Nigeria, Botswana, Ghana, and South Africa [3–6]. Most disposal sites are not properly planned, thus environmental monitoring is mandatory to ascertain the conditions of landfill sites with a view to gain the knowledge of possible interaction with the environment.

The environmental challenges of landfills include contamination of groundwater by pollutants, migration of the pollutants away from the site via surface run-off, groundwater or through release into the atmosphere [7]. The most common approach for investigating leachate plume migration from a dumpsite is to drill a network of monitoring wells around the site. However, these wells are expensive to construct and maintain [8]. In addition, limited information on subsurface hydrogeology and/or budget limitations frequently compels the citing of monitoring wells at random [9]. This approach is both technically and economically inefficient because "monitoring wells give point measurements, whereas leachate plumes tend to migrate along preferential pathways, determined by subsurface heterogeneity" [8]. The application of noninvasive and affordable geophysical techniques, such as electrical resistivity imaging (ERI), Induced polarization methods, Electrical

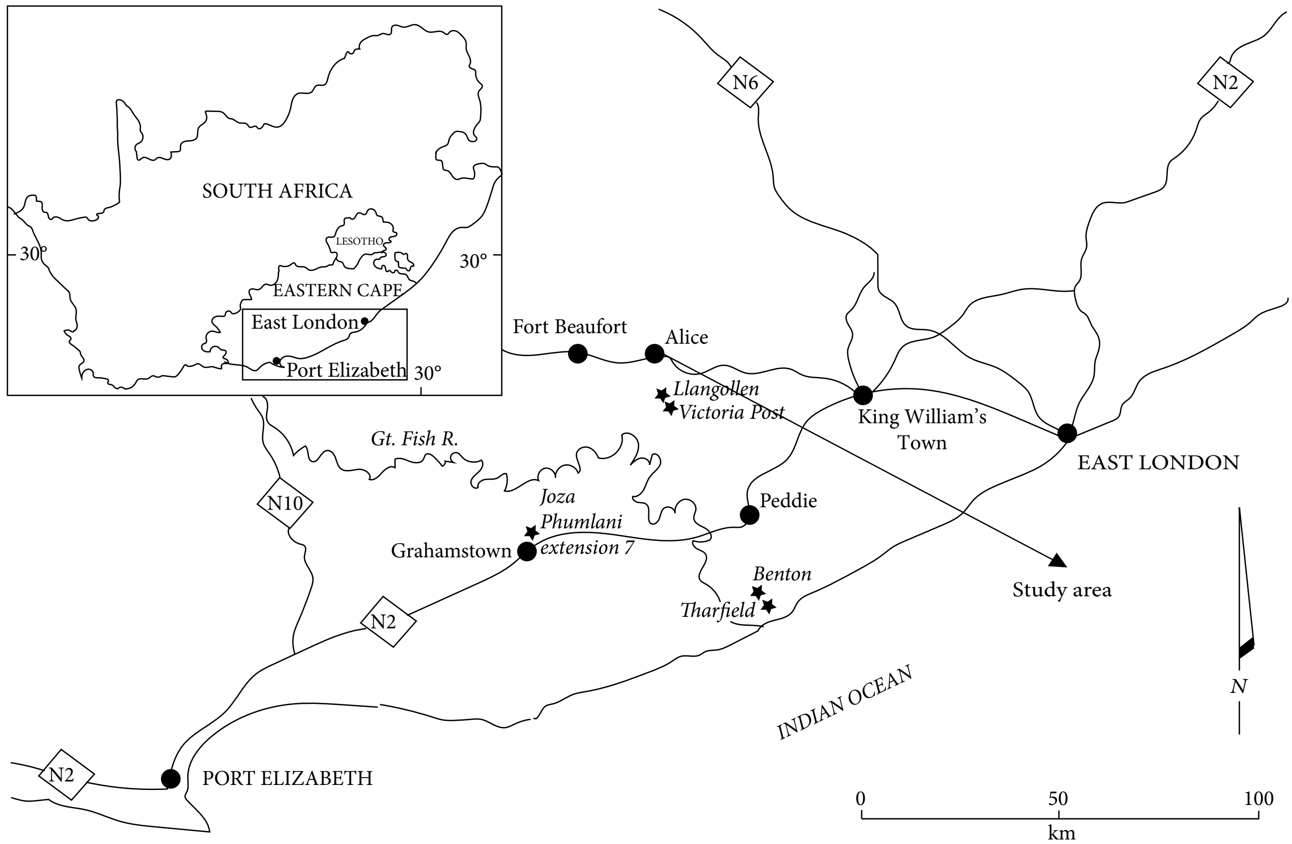

Figure 1: Map of the Eastern Cape Province showing the study area.

Conductivity (EC) logging, and seismic surveys, for delineating the occurrence and movement of leachate and for facilitating decision making regarding the location of monitoring wells have been used over the years [10]. This study focussed on the use of electrical geophysical method involving the 2D electrical resistivity and induced polarization (IP) technique to map possible leachate distribution and migration processes from the landfill site in Alice Town, Eastern Cape Province of South Africa. Subsurface geology is interpreted based on electrical resistivity measurement and IP chargeability. Detailed information about the nature of waste in a landfill is an important factor in the determination of the effective remediation approach towards mitigating the effects of the contaminants and also as a reference in planning for prospective landfill areas.

IP and resistivity methods are fast and cost effective. Resistivity methods have already been shown to be useful in delineating some landfills where there is a sharp contrast between the landfill and the background material [3]. In landfills where there is moderate or low resistivity contrast between the landfill material and the background, landfill material can be mistaken for back-filled excavations [11, 12]. This similarity in resistivity contrast with the native background, can be easily confused.

The combination of resistivity and time-domain induced polarization (IP) has been shown to be a powerful tool to obtain an overview of landfills [13, 14]. The specific objectives of this study is to delineate the lithology, layered parameters (resistivity and thicknesses), identify possible contaminant leachate plumes and the potential risk to groundwater due to the landfill by estimating the depth of contamination into the aquiferous zone. This will enable appropriate recommendation about the conditions of the landfill to be made from the geophysical results obtained.

1.1. Location of the Study Area. The study area is located in the Eastern Cape Province (Figure 1), which lies on the south eastern seaboard of South Africa. It covers an area of approximately 170 000 km^2, representing about 14% of South Africa's landmass [15]. Despite the existence of a range of alternative disposal technologies, waste management services in the Eastern Cape Province rely heavily on landfills and dump sites for the disposal of waste, which account for the majority of licensed waste facilities [16]. Waste disposal facilities like landfill sites, waste storage facilities, recycling facilities, materials recovery facilities, and waste transfer facilities are crucial indicators in determining where municipal solid waste material ends up.

DEAT [17] reported that there are 101 operational waste disposal sites in the Eastern Cape Province, 74 sites reported from questionnaires, 7 sites from permitting records and 20 sites estimated by projection. It is estimated that only 8% of landfills in the Eastern Cape Province complied with Department of Water Affairs and Forestry (DWAF) minimum requirements, 54% could potentially comply and 38% are currently unacceptable [18]. The Alice solid waste disposal site is

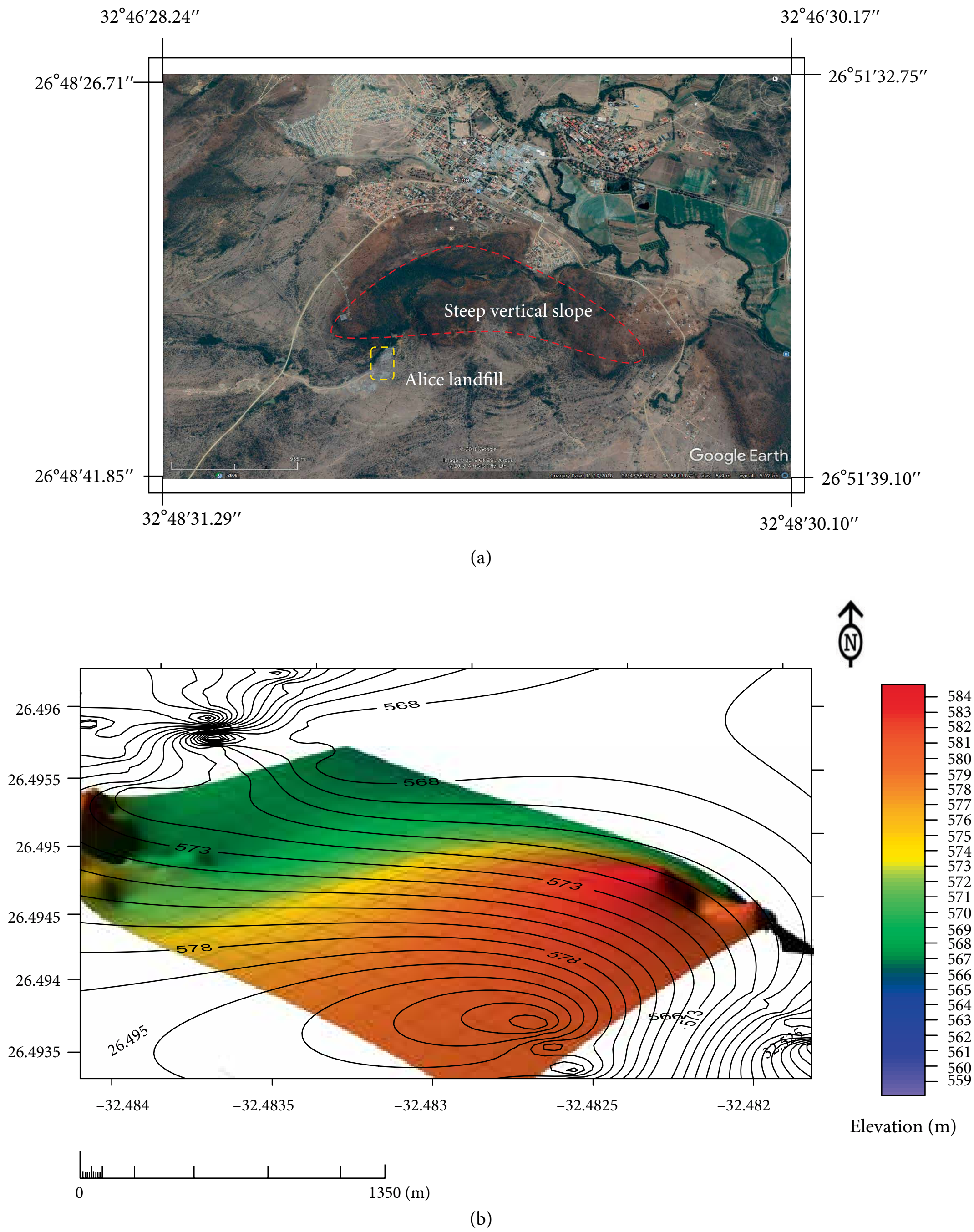

Figure 2: (a) Satellite image of the Alice area showing the landfill site (source: Google earth images). (b) 3-D contoured elevation map of the landfill.

located between latitudes S 32°48′ 26.7″–S 32°48′ 19″ and longitudes E 26°49′ 31.5″–E 26°49′ 34.1″. The area extent is approximately 300 m by 120 m, approximately 6 km southwest of the town centre in the Eastern Cape. It is about 2 km from the Happy Rest residential area. The site which was formerly a quarry, was converted into a dumpsite in 1999. Google Earth images from of the Alice area showed a darker tone around the landfill area due to less reflection of light thus indicating an elevated area around the landfill site. This elevated point is characterised by a steep vertical ridge (Figure 2(a)), having two opposing slopes, dipping at the same angles. The long axis of this slope is shown by the sparse vegetation at the top of the ridge (Figure 2(a)). The 3-D contoured elevation map of the Alice landfill site showed ground elevation range between 559 m and 584 m across the landfill, suggesting a steep topography with the direction of the dip trending northwest –southeast from the foot of the steep vertical slope (Figure 2(b)).

The dumpsite is licensed to the Nkonkobe Municipality by the Department of Water Affairs and Forestry (DWAF) to utilise the quarry for disposing of solid waste. The site is

(a) (b)

Figure 3: (a) Alice landfill showing the classification. (b) Surface composition of the landfill.

registered with the (DWAF) as General, Communal, leachate producing (G : C : B) landfill, according to the standard minimum requirements [18, 19] (Figure 3). The site is fenced but has a broken gate. The guardroom has been vandalised and is no longer functional.

A 2 m high perimeter fence that was installed around the site for access control and breaks for wind-blown litters has been destroyed, thus resulting in unrestricted access to the site. From visual inspection, the needed systems for the regulation of the operations of a standard landfill site such as leachate collection and groundwater monitoring systems, erosion and drainage pathways [18] were also conspicuously absent at the Alice disposal site.

2. Geology

The study area is geologically located within the Karoo Supergroup. The Karoo Supergroup developed from the Gondwana Supercontinent [20]. This is supported by the similarities in strata of the Carboniferous to Jurassic period in all the continents and islands of the Southern Hemisphere [21]. Other groups under the Karoo Super group include;

(i) The Dwyka group: this is the earliest and lowest of the Karoo supergroup of sedimentary deposits. They consist of diamictite, varved shale, and mudstone [22]. The total thickness of the group is about 600–700 m.

(ii) Ecca group: this consist largely of shale and turbidites.

(iii) Beaufort group: it is composed of a monotonous sequence of shale and mudstone with some interbedded sandstone [23].

(iv) Stormberg group: stromberg group contains fossil remains with a remarkable array of insect and plant fossil found in the strata.

(v) Drakensberg group: forms the uppermost layer of the Karoo super group, forming about 1400 m of the great escarpment. It consists mainly of dolerite sills at various depths [23] (Table 1).

The Alice dumpsite falls in the Beaufort Group (Table 1), consisting of fine-grained sandstones and mudstones that show fining-upward sequence [24]. The study area is geologically within the Daggaboersnek member in the Balfour formation of the Beaufort group. The Balfour formation is a fining-upward sequence of greenish-grey sandstones with bands of darker mudstones. These members are distinguished based on the lithological variation, which is characterised by the alternating sequence of sandstones and mudstones (Table 1). The local geology of the landfill site consists of superficial deposits of alluvium. The Balfour formation sediments have been extensively intruded and baked by dolerite sills in the early Jurassic [25]. The bedrock formation is made up of dolerite sills, which are more pronounced at the northern parts of the landfill site.

3. Materials and Methods

The combined electrical resistivity and induced polarization methods involving vertical electrical sounding (VES) and Dipole-dipole measurements along profile lines was carried out on the dumpsite. 1-D measurements were taken with the GEO-METRICS (model G-41) electrical resistivity meter, while 2-D measurements were taken with the ABEM SAS 1000 Terrameter. Four Dipole-dipole traverse lines (G-J) were established at spacing intervals of 70 m (Figure 3). Each traverse line is about 100 m in length in the W-E direction. Two vertical electrical sounding (VES 1and 2) profiles each of length 200 m and trending N-S were established perpendicular to the strike of the dipole-dipole traverses (Figures 4 and 5).

Time domain induced polarization was measured at initial delay of 0.01 s, base IP interval of 100 ms, variable output current mode with an acquisition time of 0.5 s and incremental value of measurement of 1. The dipole-dipole electrode configuration was chosen for its lateral resolution and depth of penetration [26]. The raw data was filtered to remove bad measurements. The obtained 2-D resistivity data were then processed using DIPRO inversion software. The program uses the least—squares inversion scheme to minimize the

Table 1: Lithostratigraphy of the Karoo supergroup in the Eastern Cape Province compiled by the council for geoscience [19].

Supergroup	Group	Subgroup	Formation	Member	Lithology
Karoo	Stormberg		Drakensberg		Basalt, pyroclast deposits
			Clarens		Sandstone
			Elliot		Mudstone, sandstone
			Molteno		Sandstone, khaki shale, coal measures
	Beaufort	Tarkastad	Burgersdop		Mudstone, sandstone, shale
			Katberg		Sandstone, mudstone, shale
		Adelaide	Balfour	Palingkloof	Mudstone, sandstone, shale
				Elandsberg	Sandstone, siltstone
				Barberskrans	Sandstone, khaki shale
				Daggaboersnek	Shale, sandstone, siltstone
				Oudeberg	Sandstone, Khaki shale
			Middleton		Shale, sandstone, mudstone
	ECCA		Koonap		Sandstone, mudstone
			Waterford		Sandtone, shale
			Fort Brown		Shale, sandstone
			Ripon		Sandstone, shale
			Collingham		Shale, yellow claystone
			Whitehill		Black shale, chert
			Prince Albert		Khaki shale
			Dwyka		Diamictite, tillite, shale

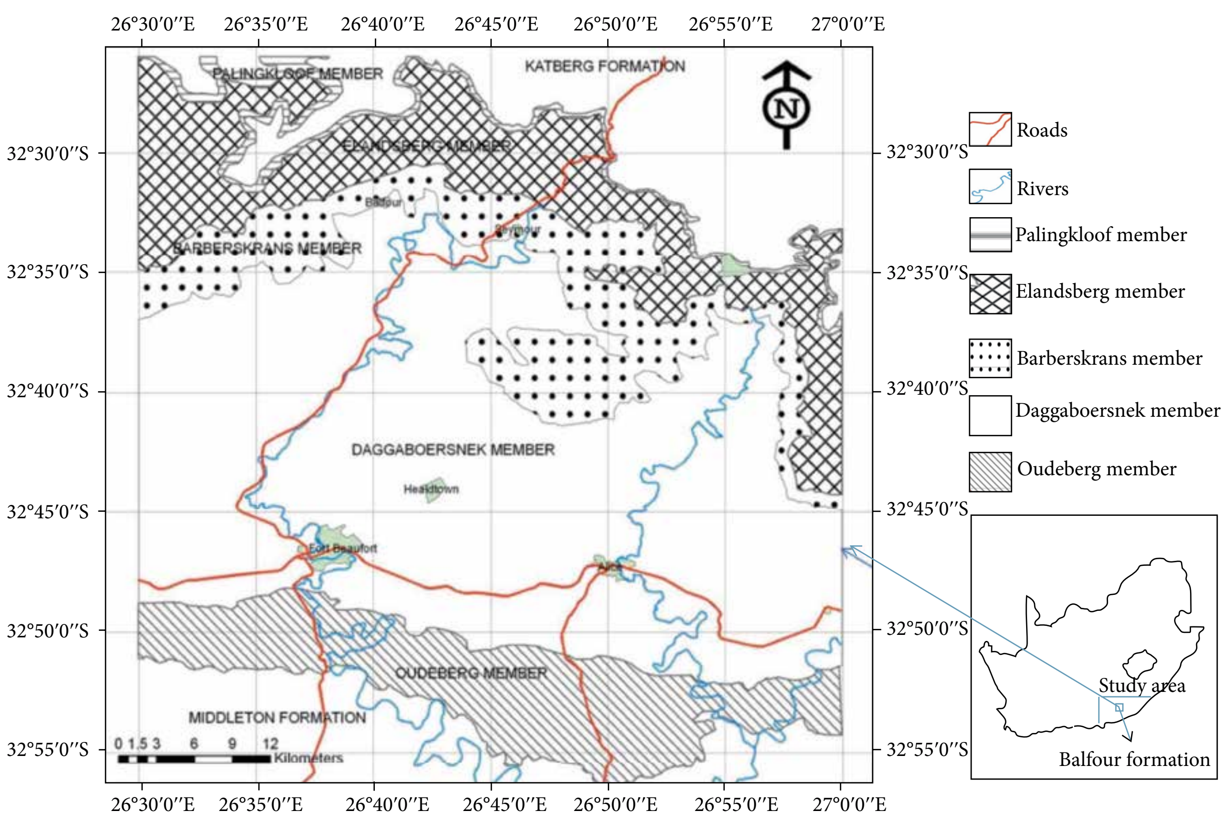

Figure 4: Map showing the distribution of sediments of the Oudeberg, Daggaboersnek, Barberskrans, Elandsberg, and Palingkloof members of the Balfour formation (modified after Katemaunzanga and Gunter [30], Baiyegunhi and Gwavava [31]).

difference between the calculated and measured apparent resistivity values, by iterative process. The results are displayed as inverted sections of the true resistivity of the subsurface rocks (Figures 6–9). Thereafter, the sections were visually inspected to delineate areas of anomalously high or low resistivities related to subsurface structures. The VES method

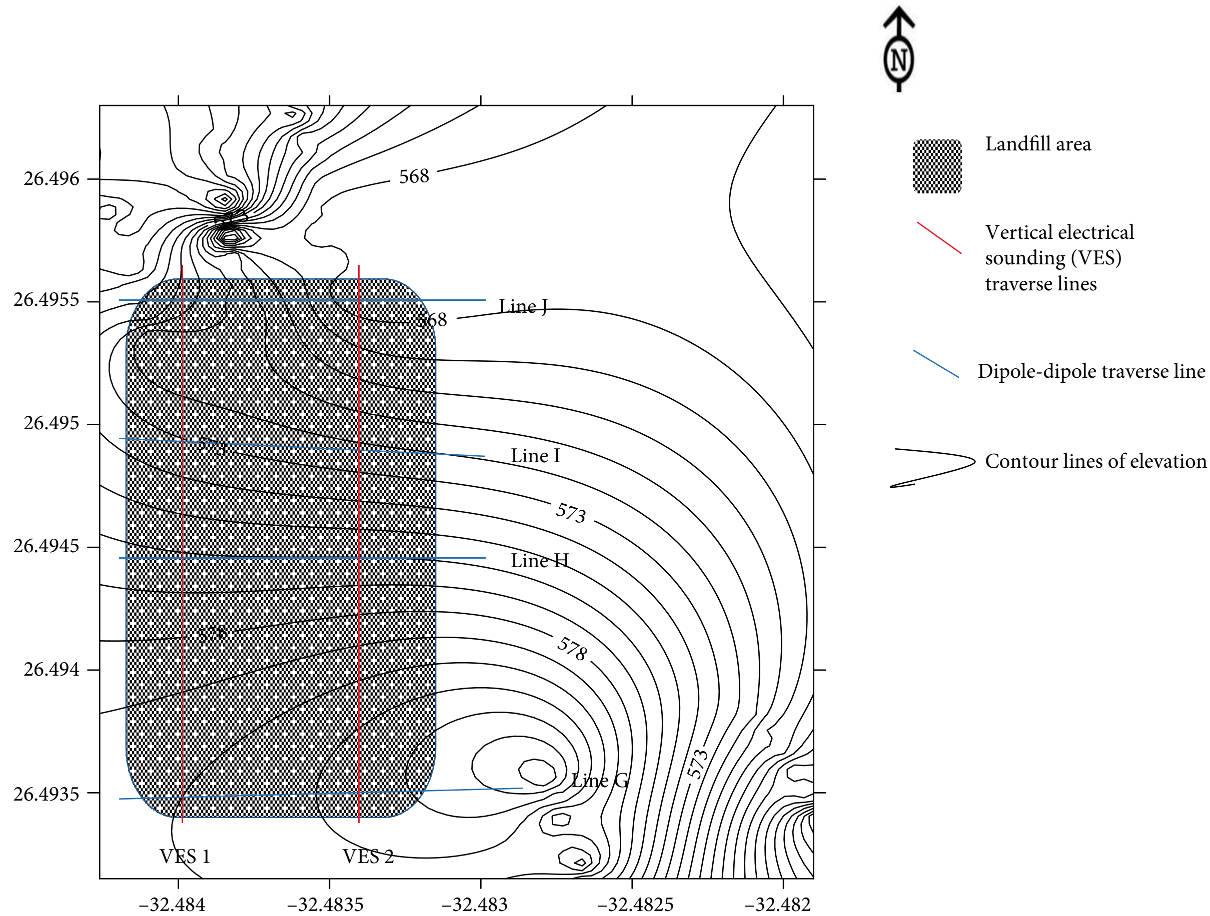

Figure 5: Geophysical data acquisition map of the Alice landfill site.

employed the Schlumberger array with a maximum current spread (AB/2) of 100 m and maximum potential spread (MN/2) of 3 m. Measured resistivity values were plotted against the current electrode separation (AB/2) and the results obtained were interpreted through visual inspection and computer inversion.

4. Results

4.1. Vertical Electrical Sounding (VES). The geoelectric resistivity section of the variation in resistivity with depth at four stations each at 50 m apart along VES 1 inside the landfill is given below;

The lithology was interpreted based on the background geology corresponding to the various resistivity range for each layer. The top layer has a resisitivty range of 4–11 Ohm-m. The mudstone formation ranged between 49.9 and 169 Ohm-m, while the weathered layer has resistivty values between 38.4 and 201 Ohm-m. The competent rock, primarily consisting of dolerite as observed from the foot of the vertical steep slope in the landfill vicinity has resisitivty values between 203 and 4660 Ohm-m.

The geoelectric resistivity section of the variation in apparent resistivity with depth at four stations each at 50 m apart along VES 2 inside the landfill is presented in Figure 10 and Table 2.

4.2. Dipole-Dipole Resistivity and Induced Polarization. The results of the dipole-dipole resistivity and chargeability measurements in the time domain along 4 selected traverses (G-J) are shown in Figures 6–9.

5. Discussion

5.1. Line G. Resistivity distribution along line G showed low resistivity values near the top layers and increasing values of resistivity with depth which also corresponds to the chargeability section along this line.

Line G apparent resistivity pseudosection (Figure 7(a)) shows a percolating leachate plume between 50 and 100 m up to a depth of about 5 m, permeating the top and the weathered layer, as shown by the blue colour legend. The average resistivity of the plume contaminated area is about 80 Ohm-m. The weathered layer (green colour) has an average resistivity of 280 Ohm-m and occurred between 5 and 15 m depth on the section. The basement rocks with high resistivity (>1000 Ohm-m) occurred within a depth range of about 15 m or more, between 20 and 70 m on the pseudosection. Line G

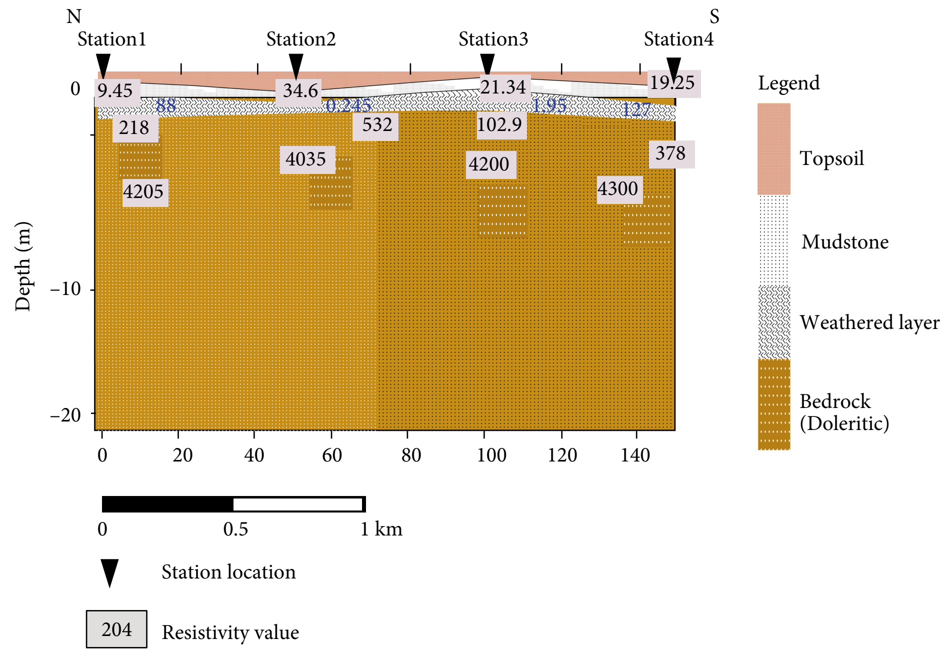

Figure 6: Geoelectric section for VES 2 showing the layer resistivities.

Table 2: Layer parameters with resistivity, thickness and depth for VES 2.

Station no	Type of curve	Layers	Resistivity (ohm-m)	Thickness (m)	Depth (m)	Lithological units
1	A-type	4	9.45	0.345	0.345	Topsoil
			188	0.377	0.722	Mudstone layer
			218	2.11	2.83	Weathered layer
			4205	∞	∞	Fresh basement
2	HA-type	4	34.6	1.188	1.188	Topsoil
			24	0.115	1.304	Mudstone
			532	0.09	1.31	Weathered layer
			4053	∞	∞	Fresh basement
3	KQ-type	4	21.34	0.183	0.183	Topsoil
			195	0.38	0.566	Mudstone
			102.9	1.314	1.881	Weathered layer
			4200	∞	∞	Weathered layer
4	A-type	4	19.25	0.62	0.62	Topsoil
			127	0.663	1.29	Mudstone layer
			378	1.26	2.54	Weathered layer
			4300	∞	∞	Fresh basement

chargeability pseudosection (Figure 7(b)) showed that high chargeability values between 90 and 100 m observed on the section, corresponded to low values on the resistivity section (Figure 7(a)). This suggests the dense nonaqueous nature of the contaminants observed in that portion on the resistivity pseudosection. This is because low resistivity values usually indicate a saturated ground while the high chargeability suggests a dense (probably) metallic contaminant in that portion, on the section. Generally across the line G chargeability pseudosection, high chargeability zones corresponds to high resistivity values. Very low chargeability values around the top layer (between 110 and 130 m) with chargeability of about 0.17–0.30 ms corresponds to low resistivity, further suggesting the presence of percolating leachate plume in the unsaturated zone. This is due to the fact that low chargeability values indicate low mobility and degree of saturation of contaminants [27].

5.2. Line H. Very low chargeability zones were observed across the top layers (from left to right, starting at 40 m) on line H chargeability section (Figure 8(a)). This suggests unsaturated plume in the top layers because of the correlation with low resistivity on the resistivity section. The plumes are not distinct on the resistivity pseudosection (Figure 8(b)). This was because

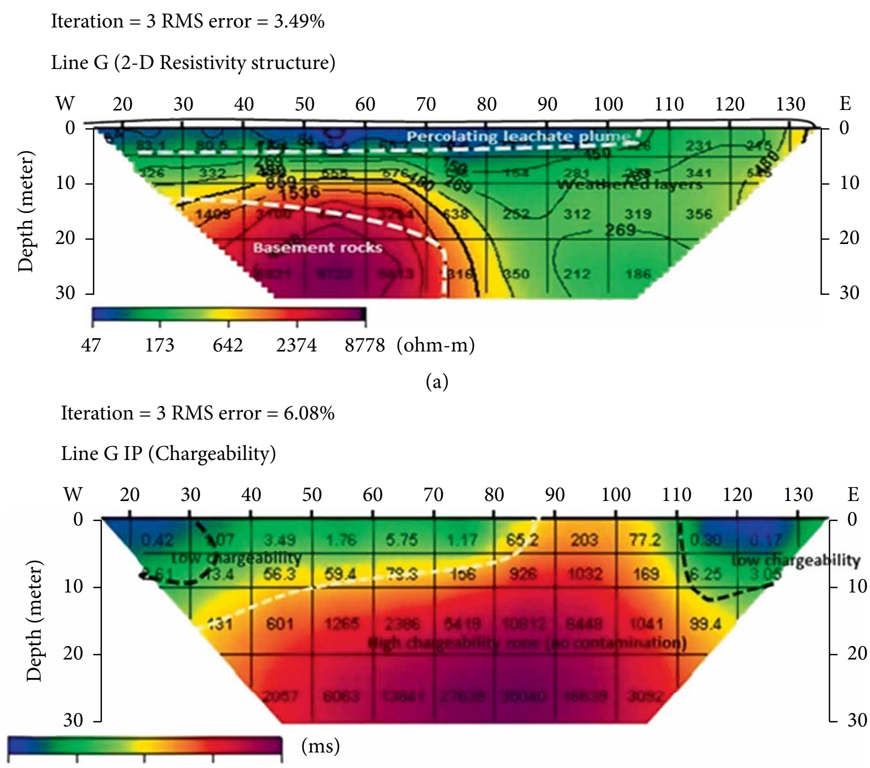

Figure 7: (a) Dipole-dipole resistivity pseudosection along line G. (b) Time domain induced polarization pseudosection along line G.

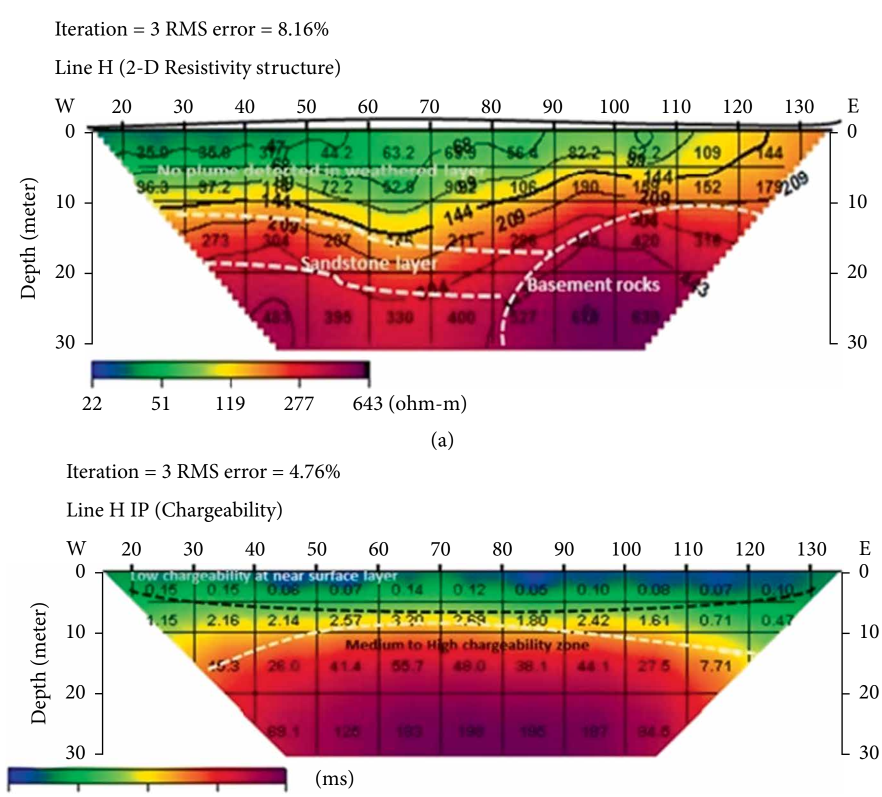

Figure 8: (a) Dipole-dipole resistivity pseudosection along line H. (b) Time domain induced polarization pseudosection along line H.

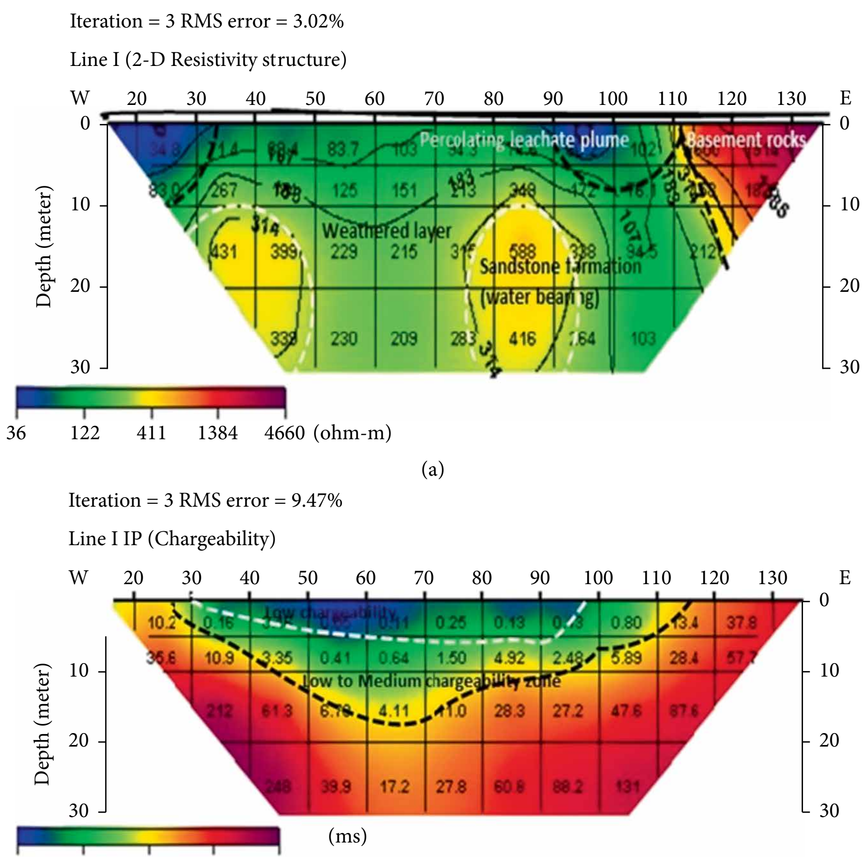

Figure 9: (a) Dipole-dipole resistivity pseudosection along line I. (b) Time domain induced polarization pseudosection along line I.

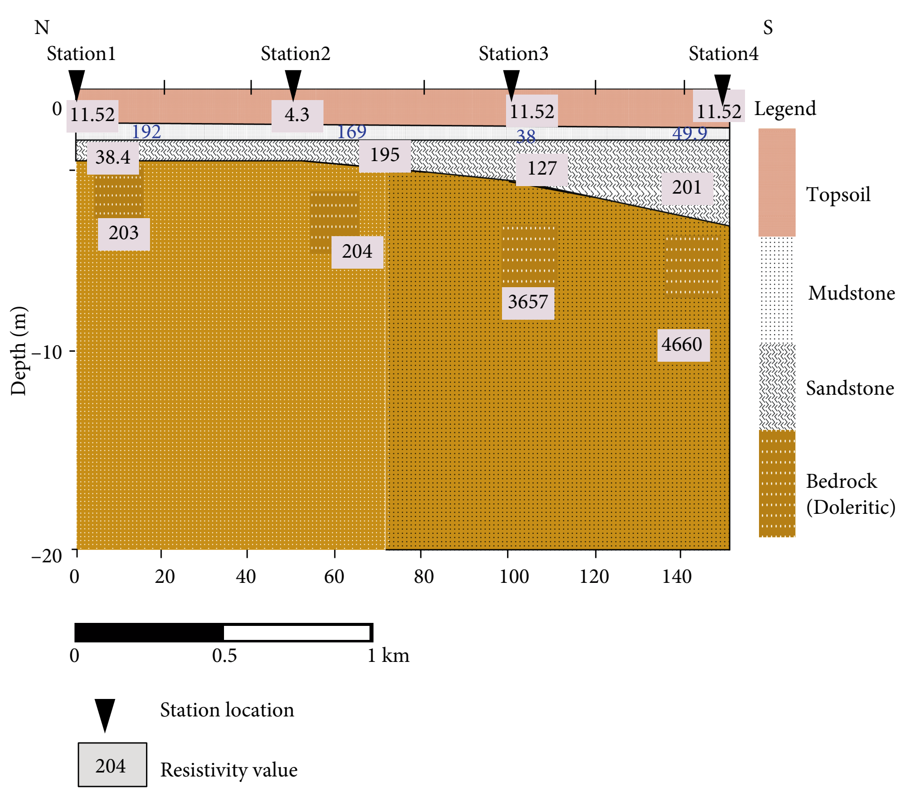

Figure 10: Geoelectric section for VES 1 showing the layer resistivities.

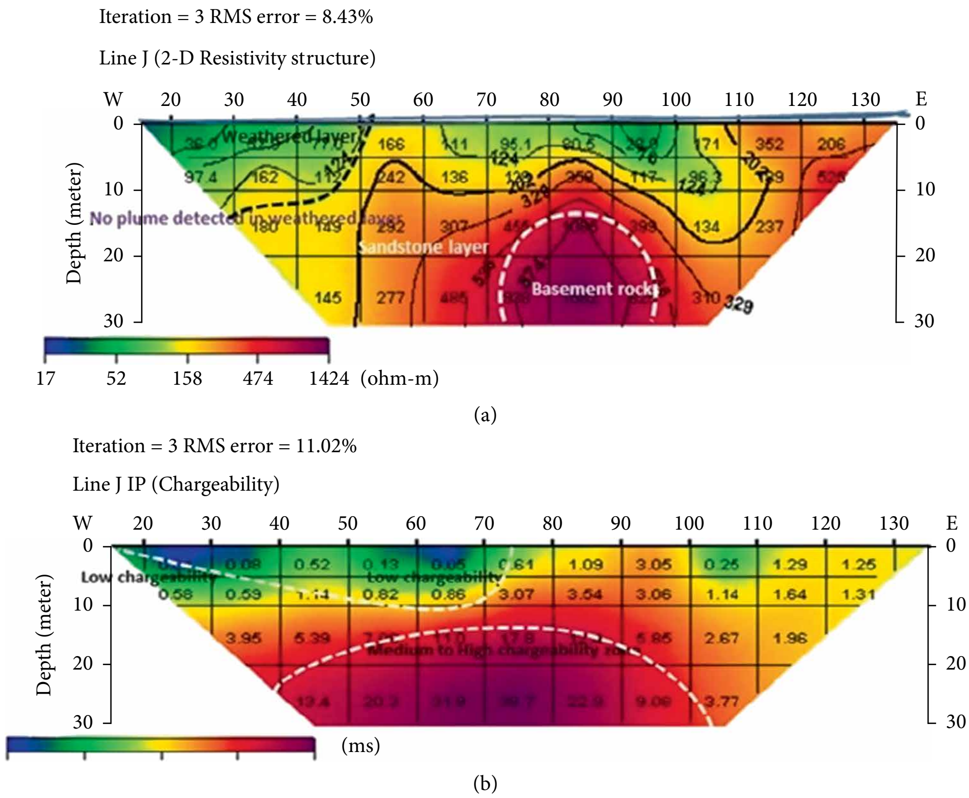

Figure 11: (a) Dipole-dipole resistivity pseudosection along line J. (b) Time domain induced polarization pseudosection along line J.

of the similar resistivity values of the leachate plume and the background formation. The values of chargeability on line H IP section was used to differentiate between the leachate plume and the background resistivity. As observed also on line G chargeability section (Figure 7(b)), high resistivity values also corresponds to high chargeability on line H (Figures 7(b), Figure 8(a)). The medium chargeability zones corresponds to the sandstone layers on the resistivity pseudosection. The apparent resistivity pseudosection along line H (Figure 8(b)), showed no evidence of leachate plume contamination around the top layers. The weathered layer occurred between 0 and 110 m and a depth of about 10 m. The sandstone layer is more pronounced on this section, occurring between 10 and 20 m depth with an average resistivity of about 267 Ohm-m, sitting atop the bedrock layers (basement rocks) which is doleritic in nature.

5.3. Line I. Line I apparent resistivity distribution pseudosection showed contaminated portions to a depth of 5 m at isolated points 20–30 m and 90–100 m respectively (Figure 9(a)). The weathered layer is more pronounced on this section, between 5 and 30 m and having an intercalation of the sandstone layer as observed on the resistivity pseudosection (Figure 9(a)). The bedrock formation occurred also at an isolated portion, between 110 and 130 m along the profile. Line I chargeability pseudosection showed low chargeability zones to a depth of about 5 m between 50 and 60 m (Figure 9(b)). This corresponds to low resistivity on the resistivity pseudosection. Percolating leachate plume observed on the resistivity pseudosection (between 90 and 100 m) (Figure 9(a)) corresponded to low values (0.13 ms) on the chargeability section. The isolated contaminated zones between 20 and 30 m observed on the resistivity pseudosection correlates to very low values on the chargeability section. This confirms the presence of two types of contaminants in the top layers-a dense nonaqueous contaminants (between 20 and 30 m) on the resistivity pseudosection with chargeability of about 10.2 ms and low resistivity of 34.9 Ohm-m and leachate plume in the unsaturated (between 90 and 100 m) on the resistivity and chargeability pseudosection with values of 30.2 Ohm-m and 0.13 ms, respectively.

5.4. Line J. Along line J pseudosection, the slightly distinct boundary between the sandstone layer and the bedrock can be observed. The basement rocks have typical high resistivities ≥1000 Ohm-m and they occurred between 80 and 100 m, while the sandstone overlies the basement. There was no leachate plume detected across the layers on the resistivity pseudosection (Figure 11(a)). Line J IP pseudosection showed very low chargeability values (0.04 ms), between 20 and 30 m (Figure 11(b)). This correspond to low values on the resistivity pseudosection (35 Ohm-m) (Figure 9(a)). This points to the dense nature of the contaminants found in this portion which has similar resistivity to the weathered layers on the resistivity pseudosection (Figure 11(a)). Generally across this section, high resistivity values correspond to high chargeability values. (Figures 11(a) and 11(b)). This suggests the bedrock layers occurring between 20 and 30 m depth across both sections.

Table 3: Layer parameters with resistivity, thickness and depth for VES 1.

Station no	Type of curve	Layers	Resistivity (ohm-m)	Thickness (m)	Depth (m)	Lithological units
1	A-type	4	11.5	0.16	0.16	Topsoil
			19.1	0.448	0.608	Mudstone layer
			38.4	0.809	1.42	Weathered layer
			203	∞	∞	Fresh sandstone layer
2	A-type	4	4.3	0.063	0.06	Topsoil
			169	0.125	0.189	Mudstone layer
			195	1.253	1.44	Weathered layer
			204	∞	∞	Fresh sandstone layer
3	A-type	4	11.52	0.723	0.723	Topsoil
			38	1.06	1.78	Mudstone layer
			127	0.814	2.59	Weathered layer
			3657	∞	∞	Fresh basement
4	A-type	4	11.52	0.42	0.42	Topsoil
			49.9	0.3	0.72	Mudstone layer
			201	4.21	4.93	Weathered layer
			4660	∞	∞	Fresh basement

The potential threats to groundwater is a function of a combination of factors such as the type and toxicity of its contaminants, direction of the groundwater flow, high permeability of the lithological layers and depth to the aquiferous zone [28]. The overlay of the vertical electrical sounding (VES) profiles on the geoelectric section from the landfill site showed a general 4-layered earth system across VES 1 and VES 2 where $\rho 1 < \rho 2 < \rho 3 < \rho 4$ (Tables 2 and 3) as deduced from the geology and resistivity values obtained from the measurements. The top layer is made up of loose coarse grained sediments with average thickness of 0.7 m and resistivity of 19.25 Ohm-m (Figure 6). This is followed by a second layer of mudstone, having layer resistivity of 74 Ohm-m and an average thickness of 0.5 m (Figure 10). The third layer, predominantly consisting of sandstone has an average resistivity of 515 Ohm-m. The bedrock layer is made up of dolerite with very high resistivity (>1000 Ohm-m) (Figures 6 and 10).

The geoelectric sections (Figures 6 and 10) showed a low depth to the top of the bedrock (<10 m). This is also corroborated on the resistivity pseudosections (Figures 7–11). The bedrock layer having high resistivity and chargeability values is conspicuous across the resistivity and IP models. The possible nature of contaminants present in the landfill were deduced from the anomalous values of resistivity and chargeability across the pseudosections. In-situ values of chargeability generally appear lower than laboratory measurements of chargeability [29]. This is because in a field situation, the current flow is often through a section of mixed materials in the earth so that the true chargeability of a material cannot be accurately determined on the field.

Line G (Figure 7(a)) apparent resistivity model indicated anomalous zones of low resistivity, corresponding to low chargeability time domain values on the IP pseudosection. This is interpreted to be percolating leachate plume in the unsaturated zone. Low IP values around the top layer on the IP pseudosection (between 110 m and 130 m) corresponded to high resistivity values. This indicates dense nonaqueous phase contaminants from dumping on the top layer because of the high values of resistivity on the corresponding section. The low chargeability values (between 40 m and 100 m) on line H (Figure 8(a)) corresponded to low resistivity on the resistivity model along the line. However, there is an absence of contaminant leachate plume on the resistivity section within the 40–100 m range. This suggests that the contaminants have similar resistivity values to the background lithology. The low to intermediate apparent resistivity zones on line I (Figure 9(a)), going from left to right, correlates to very low chargeability values near the surface on the corresponding chargeability section (Figure 9(b)).

A low resistivity section (90.2 Ohm-m) is distinct between 90 m and 100 m on line I resistivity model. The effectiveness of the combination of the induced polarization method with electrical resistivity method is demonstrated on Line I, (Figures 9(a) and 9(b)), where waste at the middle of the IP model (between 50 m and 60 m) was not detected on the resistivity section, as the top layer had uniform resistivity. This suggests the dense nonaqueous nature of the anomaly on the IP section which may have similar resistivity to the background lithology at that section. Line J (Figure 11) has low chargeability values near the surface on the IP model, correlating to low resistivity values on the resistivity section. This further confirms the presence of percolating unsaturated leachate plume on the landfill.

6. Conclusion

The results of the combination of induced polarization and electrical resistivity methods have been used to determine the electrical properties of the rock type, lithological layers, and identify the presence of possible contaminant leachate plume from the landfill in Alice, South Africa. This has also helped in reducing uncertainties that may remain in interpretations when only the electrical resistivity method is used. Low values of resistivity near the top layer on the models indicated contaminants, ranging from unsaturated waste with high ion contents to dense aqueous phase liquid contaminants. Intermediate resistivities showed layers of intermediate grainsize and texture. The high resistivity zones are the bedrock. Contaminant plumes generally appeared as low resistivity, low chargeability materials especially near the surface of the models. The shallow depth to the competent bedrock poses a low risk to groundwater contamination around the dumpsite. However the steep topography of the dumpsite due to its location at the foot of a steep vertical slope favours rapid movement of the contaminants along the surface at shallow depths. Construction of waste cells on the landfill is proffered as a remediation method for waste management around the site.

Data Availability

Collected field data for the research are available upon request at the Department of Geology, University of Fort Hare, South Africa and also from the corresponding author.

Conflicts of Interest

The authors declare that they have no conflicts of interest regarding the publication of this research work.

Acknowledgments

The authors wish to acknowledge the Buffalo City Metropolitan Municipality (BCMM) for granting access permit to the landfill site. Also, the Council for Geosciences (CGS) South Africa is appreciated for providing instrumentation for the geophysical data acquisition.

References

[1] D. S. McFarlane, J. A. Cherry, R. W. Gilham, and E. A. Sudicky, "Migration of contaminants in groundwater at a landfill: a case study," *Journal of Hydrology*, vol. 63, no. 1-2, pp. 1–29, 1993.

[2] S. Mor, K. Ravindra, R. P. Dahiya, and A. Chandra, "Leachate characterization and assessment of groundwater pollution near municipal solid waste landfill site," *Environmental Monitoring and Assessment*, vol. 118, no. 1–3, pp. 435–456, 2006.

[3] A. A. Elijah, F. F. Adetayo, and T. K. Olushola, "Integrated geophysical and geochemical methods for environmental assessment of municipal dumpsite," *International Journal of Geosciences*, vol. 4, no. 5, pp. 850–862, 2013.

[4] H. M. Jafaru, G. N. N. Dowuona, T. A. Adjadeh, E. K. Nartey, P. M. Nude, and N. Dora, "Geochemical assessment of heavy metal pollution as impacted by municipal solid waste at Abloradjei waste dump site, Accra-Ghana," *Research Journal of Environmental and Earth Sciences*, vol. 7, no. 3, pp. 50–59, 2015.ISSN: 2041–0484, e-ISSN: 2041–0492

[5] E. M. Shemang, K. Mickus, and M. P. Same, "Geophysical characterization of the abandoned Gaborone landfill, Botswana: implications for abandoned landfills in arid environment," *International Journal of Environmental Protection*, vol. 1, no. 1, pp. 1–12, 2011.

[6] R. Tshibalo, "*Assessment of municipal solid waste leachate pollution on soil and groundwater system at Onderstepoort landfill site in Pretoria*," University of South Africa, Pretoria, 2017, Master of Science dissertation in environmental science.

[7] E. Dimitriou, I. Karaouzas, I. Saratakos, I. Zacharias, K. Bogdanos, and A. Diapoulis, "Groundwater risk assessment at a heavily industrialized catchment and the associated impacts on a Peri-Urban wetland," *Journal of Environmental Management*, vol. 88, no. 3, pp. 526–538, 2008.

[8] C. Bernstone and T. Dahlin, "DC resistivity mapping of old landfills: two case studies," *European Journal of Environmental and Engineering Geophysics*, vol. 2, pp. 121–136, 1997.

[9] J. T. Zume, A. Tarhule, and S. Christenson, "Subsurface imaging of an abandoned solid waste landfill site in Norman, Oklahoma," *Groundwater Monitoring & Remediation*, vol. 26, no. 2, pp. 62–69, 2006.

[10] J. J. Butler, J. M. Healey, L. Zheng, W. McCall, and M. K. Schulmeister, "Hydrostratigraphic characterization of unconsolidated alluvial deposits with direct-push sensor technology," pp. 40–99, 1999, Kansas Geological Survey Open-File Report.

[11] Y. E. Angoran, D. V. Fitterman, and D. J. Marshall, "Induced polarization: a geophysical method for locating cultural metallic refuse," *Science*, vol. 184, no. 4143, pp. 1287–1288, 1974.

[12] N. R. Carlson, C. M. Mayerle, and K. L. Zonge, "Extremely fast IP used to delineate buried landfills," in *Proceedings of the 5th Meeting of the Environmental and Engineering Geophysical Society European Section*, EEGS, the Environmental and Engineering Geophysical Society, European Section, Lausanne, Switzerland, Budapest, Hungary, 6–9 September 1999.

[13] V. Iliceto and G. Morelli, "Environmental assessment of municipal waste dump sites with electrical resistivity and induced polarization multi electrode methods," in *Proceedings of the 5th Meeting of the EEGS (Environmental and Engineering Geophysics Society)*, EEGS, the Environmental and Engineering Geophysical Society, European Section, Lausanne, Switzerland, European Section, Budapest, Hungary, 6–9 September 1999.

[14] V. Leroux, T. Dahlin, and M. Svensson, "Dense resistivity and induced polarization profiling for a landfill restoration project at Härlöv, Southern Sweden," *Waste Management & Research*, vol. 25, no. 1, pp. 49–60, 2007.

[15] Statistics South Africa, "Census 2001: census in brief," 2003, Report No 03–02–03.

[16] SAEO, "Chapter 9 – waste management – draft 2. South Africa environment outlook. 2012. Chapter 9: waste management draft 2," 2012.

[17] DEAT, "Department of environmental affairs & tourism. Disposal sites for hazardous and general waste in South Africa," *Baseline Study in Preparation for the National Waste Management Strategy for South Africa*, DWAF, Pretoria, 1st edition, 2001.

[18] DWAF, "Department of water affairs and forestry," *Minimum Requirements for Waste Disposal by Landfill*, DWAF, Pretoria, Second edition, 1998.

[19] J. Lincoln, "South Africa; waste management, 2011," Swiss Business Hub-South Africa, Pretoria, South Africa, 2011.

[20] O. Catuneanu, P. J. Hancox, and B. S. Rubidge, "Reciprocal flexural behaviour and contrasting stratigraphies: a new basin development model for the Karoo retroarc foreland system, South Africa," *Basin Research*, vol. 10, no. 4, pp. 417–439, 1998.

[21] M. R. Johnson, C. J. van Vuuren, J. N. J. Visser et al., in *Sedimentary Rocks of the Karoo Supergroup*, M. R. Johnson, C. R. Anhaeusser, and R. L. Thomas, Eds., pp. 461–499, Pretoria, 2006, The Geology of South Africa. Geological Society of South Africa, Johannesberg /Council for Geoscience.

[22] T. Schlüter, *Geological Atlas of Africa: With Notes on Stratigraphy, Tectonics, Economic Geology, Geohazards and Geosites of Each Country*, Springer, Berlin, Germany, pp. 26–28, 2nd edition, 2008.

[23] J. F. Trustwell, *The Geological Evolution of South Africa*, Purnell, Cape Town, pp. 131–159, 1977.

[24] J. N. J. Visser, "Post-glacial Permian stratigraphy and geography of southern and central Africa: boundary conditions for climatic modelling," *Palaeogeography, Palaeoclimatology, Palaeocology*, vol. 118, pp. 213–243, 1995.

[25] A. R. Duncan and J. S. Marsh, "The Karoo igneous province," in *The Geology of South Africa*, M. R. Johnson, C. R. Anhaeusser, and R. J. Thomas, Eds., pp. 501–520, Geological Society of South Africa, Marshalltown, 2006.

[26] M. H. Loke, *Tutorial: 2-D and 3-D Electrical Imaging Surveys*, 2004, http://www.geomom.com, 2004 Revised Edition.

[27] P. Soupious, N. Papadopoulos, I. Papadopoulos et al., "Application of integrated methods in mapping waste disposal areas," *Environmental Geology*, vol. 53, pp. 661–675, 2007.

[28] S. Al-Khadi, "Assessment of groundwater contamination vulnerability in the vicinity of Abqaiq landfill-A GIS approach," King Fahd University of Petroleum and Minerals, Saudi Arabia, 2006, Dissertation.

[29] W. M. Telford, L. P. Geldart, and R. E. Sheriff, *Applied Geophysics*, Cambridge University Press, NY 11122, USA, pp. 7–103, 1982, Cap. 2.

[30] D. Katemaunzanga and G. J. Gunter, "Lithostratigraphy, sedimentology and provenance of the Balfour Formation, Beaufort Group in the Fort Beaufort Alice area, Eastern Cape Province, South Africa," *Acta Geologica Sinica (English Edition)*, vol. 83, no. 5, pp. 902–916, 2009.

[31] C. Baiyegunhi and O. Gwavava, "Variations in isochore thickness of the Ecca sediments in the Eastern Cape Province of South Africa, as deduced from gravity models," *Acta Geologica Sinica (English Edition)*, vol. 90, no. 5, pp. 1699–1712, 2016.

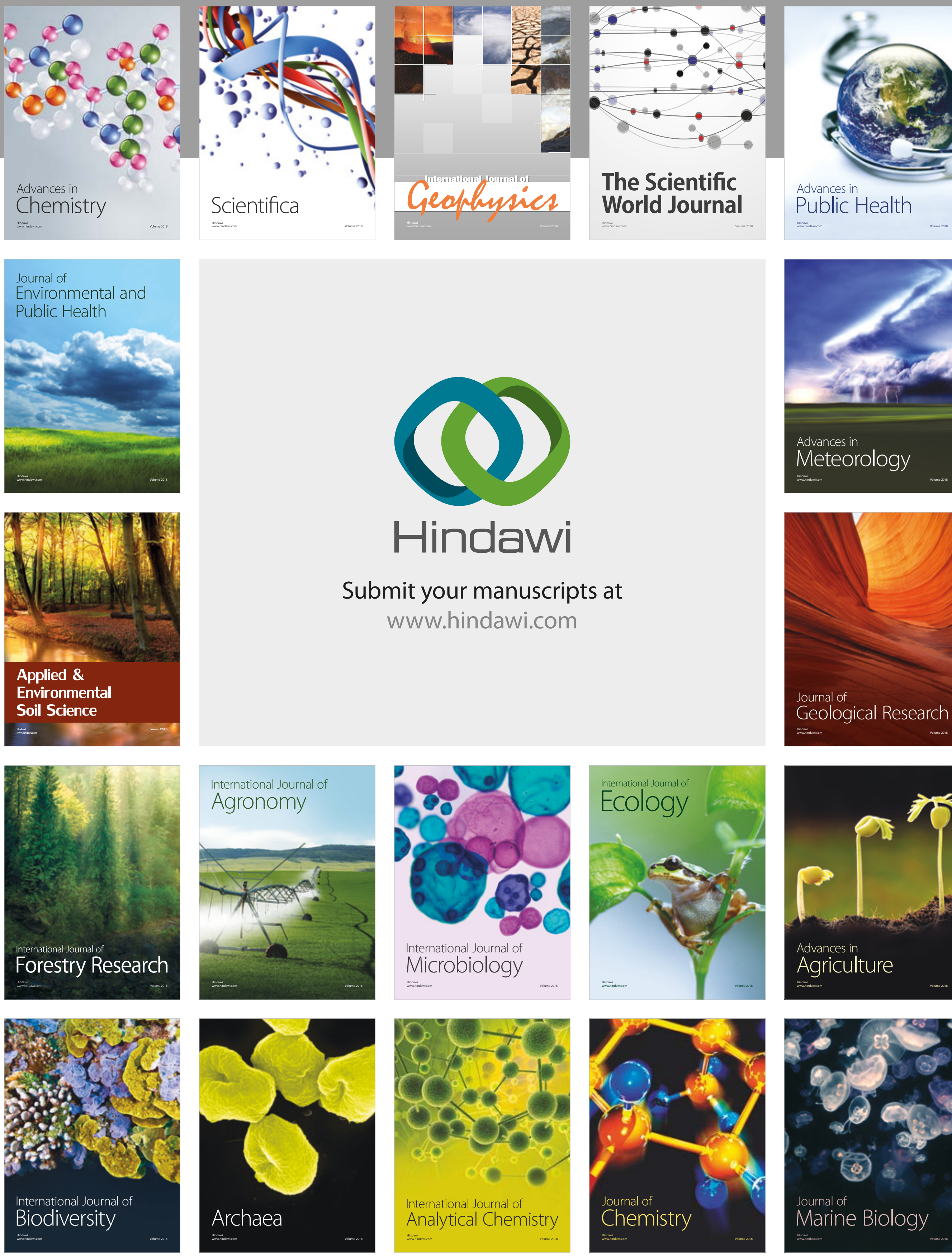
Advances in Chemistry
Scientifica
International Journal of Geophysics
The Scientific World Journal
Advances in Public Health
Journal of Environmental and Public Health
Hindawi
Submit your manuscripts at
www.hindawi.com
Advances in Meteorology
Applied & Environmental Soil Science
Journal of Geological Research
International Journal of Forestry Research
International Journal of Agronomy
International Journal of Microbiology
International Journal of Ecology
Advances in Agriculture
International Journal of Biodiversity
Archaea
International Journal of Analytical Chemistry
Journal of Chemistry
Journal of Marine Biology